Effect of far-field flow on a columnar crystal in the convective undercooled melt*

Ji Xiao-Jian(姬小建)[a], Chen Ming-Wen(陈明文)[a]†, Xu Xiao-Hua(徐小花)[a], and Wang Zi-Dong(王自东)[b]

[a] School of Mathematics and Physics, University of Science and Technology Beijing, Beijing 100083, China
[b] School of Materials Science and Engineering, University of Science and Technology Beijing, Beijing 100083, China

(Received 16 June 2014; revised manuscript received 25 August 2014; published online 25 November 2014)

The growth behavior of a columnar crystal in the convective undercooled melt affected by the far-field uniform flow is studied and the asymptotic solution for the interface evolution of the columnar crystal is derived by means of the asymptotic expansion method. The results obtained reveal that the far-field flow induces a significant change of the temperature around the columnar crystal and the convective flow caused by the far-field flow accelerates the growth velocity of the interface of the growing columnar crystal in the upstream direction and inhibits its growth velocity in the downstream direction. Our results are similar to the experimental data and numerical simulations.

Keywords: columnar crystal, far-field uniform flow, interface morphology, crystal growth

PACS: 64.70.D–, 68.08.–p, 81.30.Fb **DOI:** 10.1088/1674-1056/24/1/016401

1. Introduction

The growth behavior and pattern formation of the columnar crystal during the solidification of the undercooled melt is an important issue in the materials science and condensed matter physics and has been extensively investigated during the past years.[1–4] Coriell and Parker[5] analyzed the morphological stability of the columnar crystal undergoing diffusion-controlled growth in consideration of isotropic interfacial tension and revealed that the growth of the crystal is unstable when the radius is greater than and stable when the radius is less than the critical radius. The analogous mechanism is also found by Mullins and Sekerka.[6] Chen *et al.*[7] studied the microstructure of different positions of the columnar crystal experimentally and analyzed the process of the formation and growth of the columnar crystal in the continuous directional solidification. It is shown that the growth of the columnar crystal is affected by both the columnar crystal merge mechanism and the elimination rule. Buchholz and Engler[8] found that the deformation of the solute layer around the dendrites tips caused by the forced convection makes the columnar dendrites tips incline in the upstream direction.[9,10] In the solidification, the crystal growth will be affected by many factors, such as undercooling,[11] interface kinetics,[12] anisotropic surface tension,[13,14] flow,[15–19] etc. These experiments and numerical simulations deepen the understanding of the crystal growth. However, since the nonlinear system of the crystal growth with flow has no exact analytical solutions available generally, theoretical studies on the crystal growth with flow are relatively few. Chen *et al.*[20,21] studied the effect of the far-field flow on the interface morphology of the spherical crystal. In this paper, the effect of the convective flow caused by the far-field flow on the interface evolution of the columnar crystal is discussed by using the asymptotic expansion method, the results obtained show the interface morphology of the columnar crystal affected by the far-field flow.

2. Theoretical model

Consider the growth of an infinite columnar crystal with an initial interface radius $\bar{r}_0$ in the convective undercooled melt. We assume that the melt is an incompressible Newtonian fluid. In the undercooled melt, far from the columnar crystal the temperature is $\bar{T}_\infty$, the undercooling is $\Delta T = \bar{T}_\mathrm{M} - \bar{T}_\infty$, where $\bar{T}_\mathrm{M}(\bar{T}_\infty < \bar{T}_\mathrm{M})$ is the solidification equilibrium temperature of the pure substance. The columnar crystal is influenced by the far-field flow $\bar{U}_\infty$, which points to the cross section of the columnar crystal in the rightward direction. Let $\bar{U}$ denote the convective velocity in the liquid phase, $\bar{P}$ denote the pressure, $\bar{T}_\mathrm{S}$ and $\bar{T}_\mathrm{L}$ denote the temperatures respectively for the solid and liquid phases, $\bar{R} = \bar{R}(\theta, \bar{t})$ denote the interface of the columnar crystal, in which $\bar{t}$ represents time.

We rescale the temperature scale by ΔT, velocity scale by the characteristic velocity of the interface V, length scale by $\bar{r}_0$, time scale by $\bar{r}_0/V$, pressure scale by $\rho_\mathrm{L} V^2$, where ρ_L is the density of the melt, then we introduce the following dimensionless physical quantities:

$$T_\mathrm{L} = \frac{\bar{T}_\mathrm{L} - \bar{T}_\mathrm{M}}{\Delta T}, \quad T_\mathrm{S} = \frac{\bar{T}_\mathrm{S} - \bar{T}_\mathrm{M}}{\Delta T}, \quad U = \frac{\bar{U}}{V},$$
$$P = \frac{\bar{P}}{\rho_\mathrm{L} V^2}, \quad r = \frac{\bar{r}}{\bar{r}_0}, \quad t = \frac{\bar{t}}{\bar{r}_0/V}, \tag{1}$$

*Project supported by the Overseas Distinguished Scholar Program by the Ministry of Education of China (Grant No. MS2010BJKJ005), the National Natural Science Foundation of China (Grant No. 10972030), and the Science and Technology Support Project of Jiangxi, China (Grant No. 20112BBE50006).

†Corresponding author. E-mail: chenmw@ustb.edu.cn

© 2015 Chinese Physical Society and IOP Publishing Ltd

where $V = k_{\rm L}\Delta T/\bar{r}_0\Delta H$, $k_{\rm L}$ is the heat conduction coefficient of the liquid phase, ΔH is the latent heat of fusion per unit volume. We use coordinate (r,θ) to describe the cross section perpendicular to symmetric axis of the columnar crystal affected by the far-field flow as shown in Fig. 1.

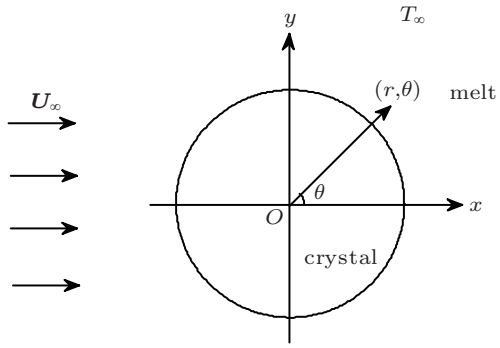


Fig. 1. A columnar crystal in the undercooled melt affected by the far-field uniform flow.

The governing equations for the convective velocity $\boldsymbol{U}$ contain the continuity equation and Navier–Stokes equation as

$$\boldsymbol{\nabla}\cdot\boldsymbol{U} = 0, \quad (r > R(\theta,t)), \tag{2}$$

$$\frac{\partial \boldsymbol{U}}{\partial t} + (\boldsymbol{U}\cdot\boldsymbol{\nabla})\boldsymbol{U} = -\boldsymbol{\nabla}P + \Omega\boldsymbol{\nabla}^2\boldsymbol{U}, \quad (r > R(\theta,t)), \tag{3}$$

where $\Omega = \upsilon/\bar{r}_0 V$, υ is the kinematical viscosity, $\boldsymbol{\nabla}$ is the gradient operator, $\boldsymbol{\nabla}^2$ is the Laplacian operator.

The convective velocity $\boldsymbol{U}$ in the far field satisfies: as $r \to \infty$,

$$\boldsymbol{U} \to \boldsymbol{U}_\infty \boldsymbol{i}, \tag{4}$$

where $\boldsymbol{U}_\infty$ is a dimensionless velocity, $\boldsymbol{i}$ is the unit vector in the positive direction of x axis.

The heat transfer processes for the temperature fields are governed by thermal conduction equations

$$\varepsilon\left(\frac{\partial T_{\rm L}}{\partial t} + (\boldsymbol{U}\cdot\boldsymbol{\nabla})T_{\rm L}\right) = \boldsymbol{\nabla}^2 T_{\rm L}, \quad (r > R(\theta,t)), \tag{5}$$

$$\varepsilon\frac{\partial T_{\rm S}}{\partial t} = \kappa\boldsymbol{\nabla}^2 T_{\rm S}, \quad (r < R(\theta,t)), \tag{6}$$

where

$$\varepsilon = \frac{\Delta T}{\Delta H/(c_{\rm p}\rho_{\rm L})}, \quad \kappa = \frac{\kappa_{\rm S}}{\kappa_{\rm L}},$$

where $c_{\rm p}$ is the specific heat, $\kappa_{\rm S}$ and $\kappa_{\rm L}$ are, respectively, the thermal diffusivities of the solid and liquid phases.

At the interface $r = R(\theta,t)$, the temperature satisfies the following Gibbs–Thomson condition and energy conservation condition:

$$T_{\rm L} = T_{\rm S} = 2\Gamma K - C^{-1}MU_{\rm I}, \tag{7}$$

$$U_{\rm I} = k\frac{\partial T_{\rm S}}{\partial n} - \frac{\partial T_{\rm L}}{\partial n}, \tag{8}$$

where

$$\Gamma = \frac{\gamma\bar{T}_{\rm M}}{\bar{r}_0\Delta H\Delta T}, \quad C = \frac{\Delta T}{\bar{T}_{\rm M}}, \quad M = \frac{V}{\mu\bar{T}_{\rm M}}, \quad k = \frac{k_{\rm S}}{k_{\rm L}},$$

and K is the local mean curvature at the interface, $U_{\rm I}$ is the growth velocity of the interface, n is the unit exterior vector normal to the crystal–melt interface, γ is the isotropic surface energy, μ is the interfacial kinetics coefficient, $k_{\rm S}$ is the heat conduction coefficient of the solid phase.

The temperature for the liquid phase $T_{\rm L}$ in the far field satisfies: as $r \to \infty$,

$$T_{\rm L} \to -1. \tag{9}$$

The initial condition of the interface is

$$R(\theta,0) = 1. \tag{10}$$

We consider the case of small undercooling or large latent heat, thus the parameter ε is very small, then the columnar crystal growth system (2)–(10) becomes a singularly perturbed boundary problem.

3. Asymptotic solution

For the case of the small parameter, we seek the asymptotic expansion solutions for the growth system (2)–(10) as $\varepsilon \to 0$,

$$\begin{aligned} &\boldsymbol{U} = \boldsymbol{U}_0 + \varepsilon\boldsymbol{U}_1 + \cdots, \quad P = P_0 + \varepsilon P_1 + \cdots, \\ &T_{\rm L} = T_{\rm L0} + \varepsilon T_{\rm L1} + \cdots, \\ &T_{\rm S} = T_{\rm S0} + \varepsilon T_{\rm S1} + \cdots, \quad R = R_0 + \varepsilon R_1 + \cdots. \end{aligned} \tag{11}$$

Substituting Eq. (11) into Eqs. (2)–(10) and expanding the interface curvature into

$$2K = -\frac{1}{R_0} + \frac{\varepsilon}{R_0^2}\left(\frac{\partial^2}{\partial\theta^2} + 1\right)R_1 + \cdots, \tag{12}$$

we equate the coefficients of like powers of ε and derive each order approximation in Eq. (11).

If $\partial/\partial t = 0$ is assumed, we obtain the leading order terms for the flow field and temperature fields satisfying

$$\boldsymbol{\nabla}\cdot\boldsymbol{U}_0 = 0, \tag{13}$$

$$(\boldsymbol{U}_0\cdot\boldsymbol{\nabla})\boldsymbol{U}_0 = -\boldsymbol{\nabla}P_0 + \Omega\boldsymbol{\nabla}^2\boldsymbol{U}_0, \tag{14}$$

$$\frac{\partial^2 T_{\rm L0}}{\partial r^2} + \frac{1}{r}\frac{\partial T_{\rm L0}}{\partial r} = 0, \tag{15}$$

$$\frac{\partial^2 T_{\rm S0}}{\partial r^2} + \frac{1}{r}\frac{\partial T_{\rm S0}}{\partial r} = 0. \tag{16}$$

At the interface $r = R_0(t)$, the interface conditions satisfy

$$\boldsymbol{U}_0 = \boldsymbol{0}, \tag{17}$$

$$T_{\rm L0} = T_{\rm S0} = -\frac{\Gamma}{R_0} - C^{-1}M\frac{{\rm d}R_0}{{\rm d}t}, \tag{18}$$

$$\frac{{\rm d}R_0}{{\rm d}t} = k\frac{\partial T_{\rm S0}}{\partial r} - \frac{\partial T_{\rm L0}}{\partial r}. \tag{19}$$

The leading order term of the temperature field for the liquid phase T_{L0} in the far field satisfies: as $r \to \infty$,

$$T_{L0} \to -1. \tag{20}$$

The initial condition is

$$R_0(0) = 1. \tag{21}$$

Approximatively, we replace $(\boldsymbol{U}_0 \cdot \boldsymbol{\nabla})\boldsymbol{U}_0$ in Eq. (14) by $(\boldsymbol{U}_\infty \cdot \boldsymbol{\nabla})\boldsymbol{U}_0$, where $\boldsymbol{U}_\infty = (\boldsymbol{U}_\infty \cos\theta, -\boldsymbol{U}_\infty \sin\theta)$. Then the solution $\boldsymbol{U}_0$ of Eq. (14) is decomposed into

$$\boldsymbol{U}_0 = -\chi \boldsymbol{i} + \boldsymbol{\nabla}\left(\varphi + \frac{1}{2b}\chi\right), \tag{22}$$

where φ and χ satisfy respectively

$$\boldsymbol{\nabla}^2 \varphi = 0, \tag{23}$$

$$\chi = -\boldsymbol{U}_\infty + \mathrm{e}^{br\cos\theta} Y, \tag{24}$$

where Y is the solution of the Helmholtz equation $\boldsymbol{\nabla}^2 Y - b^2 Y = 0$, b is subject to $\Omega/U_\infty = 1/2b$. The solution of Eq. (23) is

$$\varphi \approx B_0 \ln r + B_1 \frac{\cos\theta}{r}, \tag{25}$$

where B_0 and B_1 are constants to be determined. By solving the Helmholtz equation, χ is expressed as

$$\chi \approx -\boldsymbol{U}_\infty - C_0\left[\ln\left(\frac{1}{2}abr\right) - br\cos\theta \ln\left(\frac{1}{2}abr\right)\right] - \frac{C_1\cos\theta}{r}, \tag{26}$$

where $a = 1.7811$, C_0 and C_1 are constants to be determined. Substituting Eqs. (25) and (26) into Eq. (22), we derive the leading order approximation solutions for the flow field $\boldsymbol{U}_0 = (u_0, v_0)$ and P_0 can be expressed as

$$\begin{aligned} u_0 &= \frac{-r^2 + R_0^2 + 2r^2(\ln r - \ln R_0)}{r^2[1 - 2(\ln(abR_0) - \ln 2)]}\boldsymbol{U}_\infty \cos\theta, \\ v_0 &= -\frac{r^2 - R_0^2 + 2r^2(\ln r - \ln R_0)}{r^2[1 - 2(\ln(abR_0) - \ln 2)]}\boldsymbol{U}_\infty \sin\theta, \\ P_0 &= -\frac{2\boldsymbol{U}_\infty^2 \cos\theta}{b[1 - 2(\ln(abR_0) - \ln 2)]r}. \end{aligned} \tag{27}$$

With Eqs. (15), (16), and the interface condition (18), we obtain the leading order approximation solutions for the temperature fields written as

$$T_{L0} = a_0(t)(\ln r - \ln R_0) - \frac{\Gamma}{R_0} - C^{-1}M\frac{\mathrm{d}R_0}{\mathrm{d}t}, \tag{28}$$

$$T_{S0} = b_{S0}(t), \tag{29}$$

where $a_0(t)$ and $b_{S0}(t)$ are functions to be determined. It is seen that as $r \to \infty$, equation (28) does not satisfy the far-field condition (20). Like Coriell and Parker,[5] we take a special treatment for the far field such that R_∞ satisfies

$$T_{L0}(r = R_\infty) = -1, \tag{30}$$

then the leading order approximation solutions for the temperature fields are expressed as

$$T_{L0} = -1 + \left(1 - \frac{\Gamma}{R_0} - C^{-1}M\frac{\mathrm{d}R_0}{\mathrm{d}t}\right)\left(1 + \frac{\ln R_0 - \ln r}{A_\lambda}\right), \tag{31}$$

$$T_{S0} = -\frac{\Gamma}{R_0} - C^{-1}M\frac{\mathrm{d}R_0}{\mathrm{d}t}, \tag{32}$$

where $A_\lambda = \ln R_\infty - \ln R_0$ and R_0 follows the ordinary differential equation

$$\frac{\mathrm{d}R_0}{\mathrm{d}t} = \frac{R_0 - \Gamma}{R_0(A_\lambda R_0 + C^{-1}M)}. \tag{33}$$

With the initial condition (21), R_0 is determined by the implicit function

$$t = \frac{1}{2}A_\lambda(R_0^2 - 1) + (A_\lambda\Gamma + C^{-1}M) \times \left[(R_0 - 1) + \Gamma\ln\left(1 + \frac{R_0 - 1}{1 - \Gamma}\right)\right]. \tag{34}$$

If $\partial/\partial t = O(1)$ and $\varepsilon \to 0$ are assumed, we obtain the first-order terms for the temperature fields satisfying

$$\boldsymbol{\nabla}^2 T_{L1} = (\boldsymbol{U}_0 \cdot \boldsymbol{\nabla})T_{L0}, \tag{35}$$

$$\boldsymbol{\nabla}^2 T_{S1} = 0. \tag{36}$$

At the interface $r = R_0(t)$, the interface conditions satisfy

$$T_{L1} = T_{S1} - \Delta G_1 R_1, \tag{37}$$

$$T_{S1} = \frac{\Gamma}{R_0^2}\left(\frac{\partial^2}{\partial\theta^2} + 1\right)R_1 - C^{-1}M\frac{\partial R_1}{\partial t}, \tag{38}$$

$$\frac{\partial R_1}{\partial t} = k\frac{\partial T_{S1}}{\partial r} - \frac{\partial T_{L1}}{\partial r} - \Delta G_2 R_1, \tag{39}$$

where

$$\begin{aligned} \Delta G_1 &= \left(\frac{\partial T_{L0}}{\partial r} - \frac{\partial T_{S0}}{\partial r}\right)_{r=R_0}, \\ \Delta G_2 &= \left(\frac{\partial^2 T_{L0}}{\partial r^2} - k\frac{\partial^2 T_{S0}}{\partial r^2}\right)_{r=R_0}. \end{aligned} \tag{40}$$

The initial condition is

$$R_1(\theta, 0) = 0. \tag{41}$$

Considering the function constitution of inhomogeneous term $(\boldsymbol{U}_0 \cdot \boldsymbol{\nabla})T_{L0}$, we seek the solutions of the following form for Eqs. (35)–(41):

$$T_{L1} = A_{L1}(r, t)\cos\theta, \tag{42}$$

$$T_{S1} = A_{S1}(t) r\cos\theta, \tag{43}$$

$$R_1 = g_1(t)\cos\theta. \tag{44}$$

Substituting Eqs. (42)–(44) into interface conditions (37)–(39), we obtain

$$A_{\mathrm{L1}}(r,t) = \frac{\boldsymbol{U}_\infty(R_0-\Gamma)}{[2(\ln(abR_0)-\ln 2)-1]\,(A_\lambda R_0+C^{-1}M)} \times\left\{\frac{r}{2}\left[1+(\ln r)^2+\ln R_0\right]-(1+\ln R_0)r\ln r-\frac{R_0^2}{2r}\left[\ln\frac{r}{R_0^2}-(\ln R_0)^2+1\right]\right\} - \frac{R_0}{r}\left(C^{-1}M\frac{\mathrm{d}g_1(t)}{\mathrm{d}t}+\Delta G_1 g_1(t)\right), \tag{45}$$

$$A_{\mathrm{S1}}(t) = -\frac{C^{-1}M}{R_0}\frac{\mathrm{d}g_1(t)}{\mathrm{d}t}, \tag{46}$$

where $g_1(t)$ satisfies the ordinary differential equation

$$\frac{\mathrm{d}g_1(t)}{\mathrm{d}t} = \frac{\boldsymbol{U}_\infty\left[1+2(\ln R_0)^2+\ln R_0^2\right](R_0-\Gamma)R_0}{[4(\ln(abR_0)-\ln 2)-2]\,[R_0+(k+1)C^{-1}M]\,(A_\lambda R_0+C^{-1}M)}. \tag{47}$$

With the initial condition (41), the solution of $g_1(t)$ is expressed as

$$g_1(t) = \boldsymbol{U}_\infty\int_1^{R_0}\frac{\left[1+2(\ln R_0)^2+\ln R_0^2\right]R_0^2\mathrm{d}R_0}{[4(\ln(abR_0)-\ln 2)-2]\,[R_0+(k+1)C^{-1}M]}. \tag{48}$$

Then, the first-order approximation solutions for the temperature fields and R_1 are, respectively, expressed as

$$T_{\mathrm{L1}} = \left\{\frac{\boldsymbol{U}_\infty(R_0-\Gamma)}{[2(\ln(abR_0)-\ln 2)-1]\,(A_\lambda R_0+C^{-1}M)}\left\{-(1+\ln R_0)r\ln r+\frac{r}{2}\left[1+(\ln r)^2+\ln R_0\right] - \frac{R_0^2}{2r}\left[\ln\frac{r}{R_0^2}-(\ln R_0)^2+1\right]\right\}-\frac{R_0}{r}\left(C^{-1}M\frac{\mathrm{d}g_1(t)}{\mathrm{d}t}+\Delta G_1 g_1(t)\right)\right\}\cos\theta, \tag{49}$$

$$T_{\mathrm{S1}} = -\frac{\boldsymbol{U}_\infty C^{-1}M\left[1+2(\ln R_0)^2+\ln R_0^2\right](R_0-\Gamma)r\cos\theta}{[4(\ln(abR_0)-\ln 2)-2]\,[R_0+(k+1)C^{-1}M]\,(A_\lambda R_0+C^{-1}M)}, \tag{50}$$

$$R_1 = g_1(t)\cos\theta. \tag{51}$$

Therefore, we obtain the first-order asymptotic solutions of Eq. (11). The corresponding growth velocity of the interface is

$$\frac{\partial R}{\partial t}\approx\frac{\mathrm{d}R_0}{\mathrm{d}t}+\frac{\varepsilon\boldsymbol{U}_\infty\left[1+2(\ln R_0)^2+\ln R_0^2\right](R_0-\Gamma)R_0}{[4(\ln(abR_0)-\ln 2)-2]\,[R_0+(k+1)C^{-1}M]\,(A_\lambda R_0+C^{-1}M)}\cos\theta. \tag{52}$$

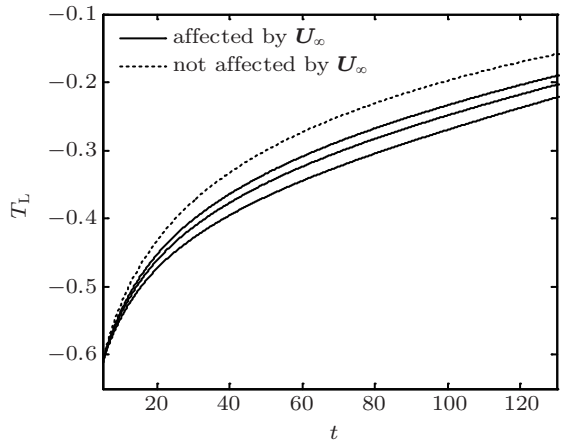


Fig. 2. The temperature variation of the liquid phase versus time t at $r=15$, where $k=1$, $C=0.3$, $M=0.09$, $\Gamma=0.01$, $\varepsilon=0.2$, $A_\lambda=3.3$, $\boldsymbol{U}_\infty=0.5$; $\theta=2\pi/3$, $3\pi/4$, π (from top to bottom for cases affected by $\boldsymbol{U}_\infty$).

With the asymptotic solution, we analyze the effect of the convective flow on the interface morphology of the columnar crystal. Figure 2 shows the temperature variation in the liquid phase along different directions. It is found that the temperature which is not affected by the far-field flow increases more remarkably than that affected by the far-field flow as time increases. Figure 3 shows the isothermal diagram of the liquid phase. The isotherm in the upstream direction where the flow comes is denser than that in the downstream direction, and the temperature variation in the upstream direction is larger than that in the downstream direction (as shown in

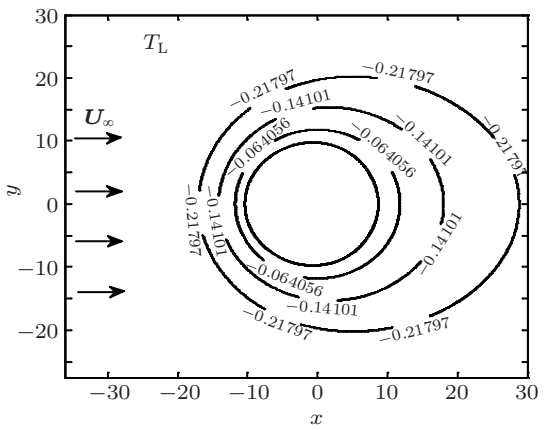


Fig. 3. The isothermal diagram of the liquid phase at $t=120$, where $k=1$, $C=0.3$, $M=0.09$, $\Gamma=0.01$, $\varepsilon=0.2$, $\boldsymbol{U}_\infty=0.5$, $A_\lambda=3.3$.

Fig. 4). Figure 5 shows that the radius of the interface affected by the flow increases more remarkably than that not affected by the flow as time increases, it implies that the far-field flow promotes the growth velocity of the interface (as shown in Fig. 6).

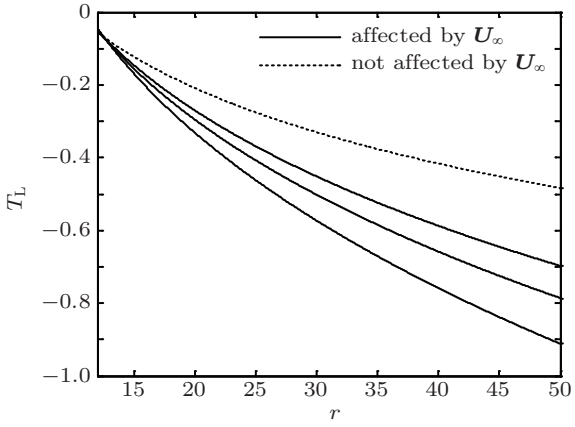


Fig. 4. The temperature variation of the liquid phase versus r at $t = 120$, where $k = 1$, $C = 0.3$, $M = 0.09$, $\Gamma = 0.01$, $\varepsilon = 0.2$, $A_\lambda = 3.3$, $\boldsymbol{U}_\infty = 0.5$; $\theta = 2\pi/3$, $3\pi/4$, π (from top to bottom for cases affected by $\boldsymbol{U}_\infty$).

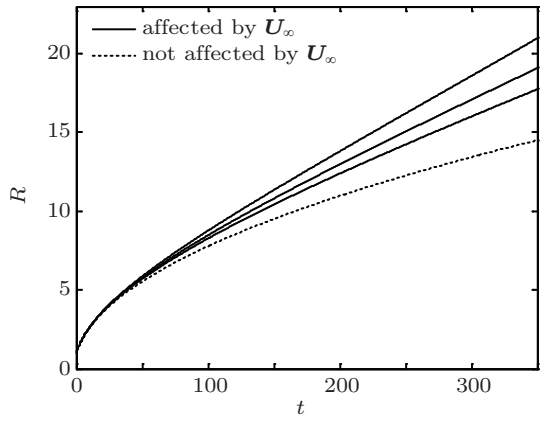


Fig. 5. The variation of the radius of the interface versus time t, where $k = 1$, $C = 0.3$, $M = 0.09$, $\Gamma = 0.01$, $\varepsilon = 0.2$, $A_\lambda = 3.3$, $\boldsymbol{U}_\infty = 0.5$; $\theta = \pi$, $3\pi/4$, $2\pi/3$ (from top to bottom for cases affected by $\boldsymbol{U}_\infty$).

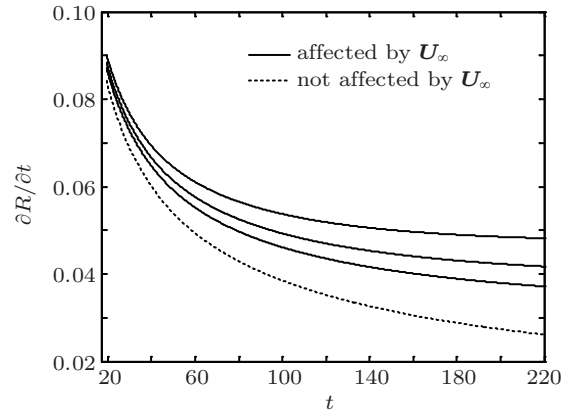


Fig. 6. The variation of the growth velocity of the interface versus time t, where $k = 1$, $C = 0.3$, $M = 0.09$, $\Gamma = 0.01$, $\varepsilon = 0.2$, $A_\lambda = 3.3$, $\boldsymbol{U}_\infty = 0.5$; $\theta = \pi$, $3\pi/4$, $2\pi/3$ (from top to bottom for cases affected by $\boldsymbol{U}_\infty$).

In the paper, we introduce the dimensionless physical quantities to simplify the equations and interface conditions, if we return to the dimensional physical quantities, we can compare qualitatively with a real system. For example, the solidification equilibrium temperature of Fe particles is $T_\mathrm{M} = 1728$ K, the undercooling of Fe particles during the solidification is $\Delta T = 373$ K, the latent heat of Fe particles per unit volume is $\Delta H = 2.404 \times 10^9$ J·m^{-3}, the specific heat is $c_\mathrm{p} = 477.3$ J·kg^{-1}·K^{-1}, the density is $\rho_\mathrm{L} = 7874$ kg·m^{-3}, $\bar{r}_0 = 1.0 \times 10^{-6}$ m, we obtain the variations of the radius and the growth velocity of the interface versus time, respectively. From Figs. 7–8, we see that the variations of the radius and the growth velocity of the interface in a real system are similar to that in the dimensionless system.

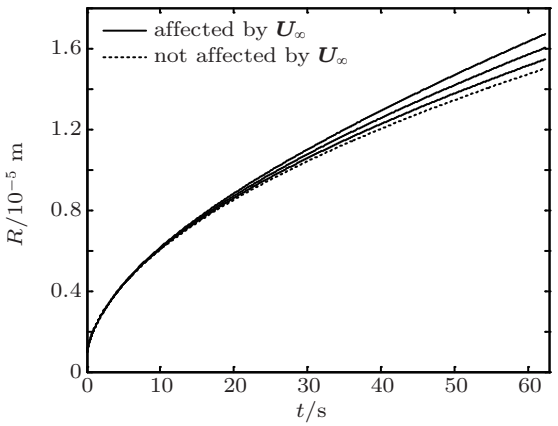


Fig. 7. The variation of the radius of the interface versus time t, where $\theta = \pi$, $3\pi/4$, $2\pi/3$ (from top to bottom for cases affected by $\boldsymbol{U}_\infty$).

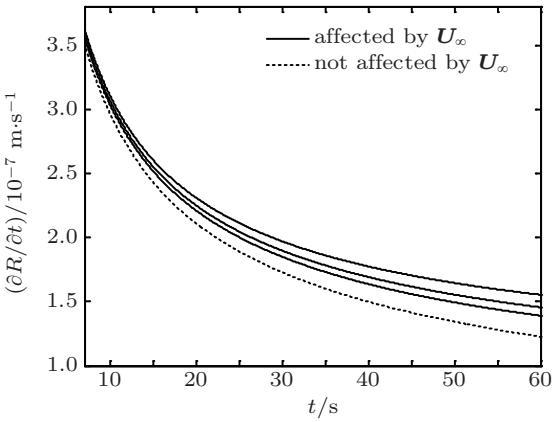


Fig. 8. The variation of the growth velocity of the interface versus time t, where $\theta = \pi$, $3\pi/4$, $2\pi/3$ (from top to bottom for cases affected by $\boldsymbol{U}_\infty$).

It is shown from the above analysis that the convective flow significantly influences the interface evolution. When $0 < \theta < \pi/2$, if $R_0 > \Gamma$, then $\mathrm{d}R_0/\mathrm{d}t > 0$, and $\partial R/\partial t < \mathrm{d}R_0/\mathrm{d}t$; if $R_0 < \Gamma$, then $\mathrm{d}R_0/\mathrm{d}t < 0$, and $\partial R/\partial t > \mathrm{d}R_0/\mathrm{d}t$. When $\pi/2 < \theta < \pi$, if $R_0 > \Gamma$, then $\mathrm{d}R_0/\mathrm{d}t > 0$, $\partial R/\partial t > 0$, and $\partial R/\partial t > \mathrm{d}R_0/\mathrm{d}t$; if $R_0 < \Gamma$, then $\mathrm{d}R_0/\mathrm{d}t < 0$,

$\partial R/\partial t < 0$, and $\partial R/\partial t < \mathrm{d}R_0/\mathrm{d}t$. It means that the convective flow accelerates the growth velocity of the interface of the growing columnar crystal in the upstream direction and inhibits its growth velocity in the downstream direction; whereas the convective flow enhances the decay velocity of the interface of the decaying columnar crystal in the upstream direction and inhibits its decay velocity in the downstream direction. Figures 9–11 show the evolution of a columnar crystal at different times (or equivalently, for different R_0) affected by the far-field flow. The theoretical results are similar to the experimental data and numerical simulations.[8]

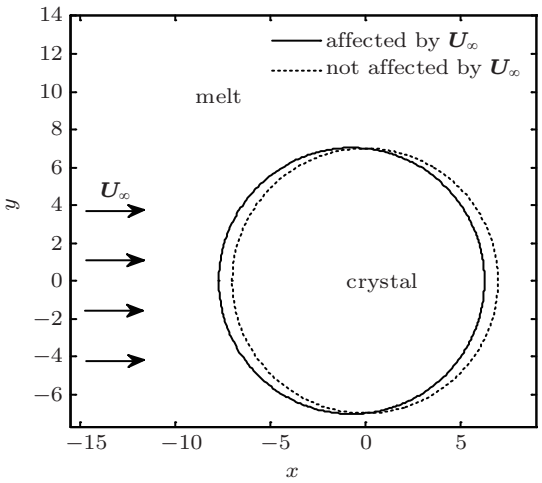


Fig. 9. The effect of the far-field flow on the evolution of a columnar crystal, where $R_0 = 7$, $U_\infty = 0.5$, $k = 1$, $C = 0.3$, $M = 0.09$, $\Gamma = 0.01$, $\varepsilon = 0.2$, $A_\lambda = 3.3$.

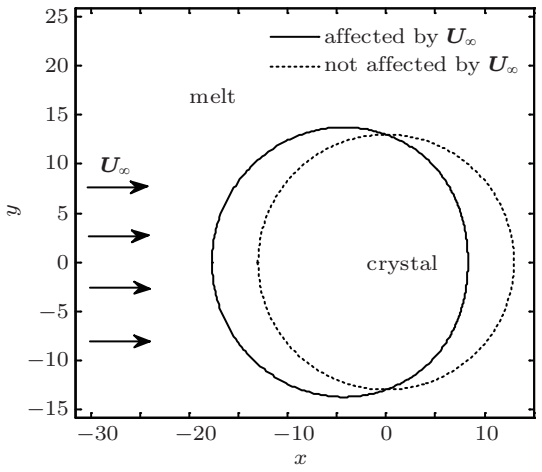


Fig. 10. The effect of the far-field flow on the evolution of a columnar crystal, where $R_0 = 13$, $U_\infty = 0.5$, $k = 1$, $C = 0.3$, $M = 0.09$, $\Gamma = 0.01$, $\varepsilon = 0.2$, $A_\lambda = 3.3$.

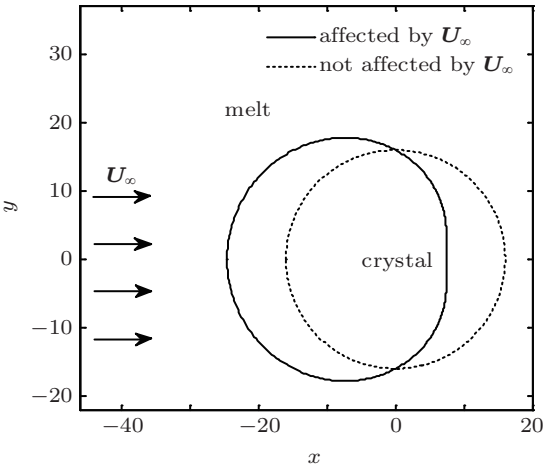


Fig. 11. The effect of the far-field flow on the evolution of a columnar crystal, where $R_0 = 16$, $U_\infty = 0.5$, $k = 1$, $C = 0.3$, $M = 0.09$, $\Gamma = 0.01$, $\varepsilon = 0.2$, $A_\lambda = 3.3$.

4. Conclusion

We investigate the growth behavior of a columnar crystal in the convective undercooled melt affected by the far-field flow and derive the approximation solution for the interface evolution by using the asymptotic expansion method. The results reveal that the far-field flow induces a significant change of the temperature around the columnar crystal and the temperature variation in the upstream direction is larger than that in the downstream direction. The convective flow accelerates the growth velocity of the interface of the growing columnar crystal in the upstream direction and inhibits its growth velocity in the downstream direction. The theoretical results are similar to the experimental data and numerical simulations.

References

[1] Mei X Y, Ma W H, Wei K X, Yang B and Dai Y N 2009 *Acta Scientiarum Naturalium Un.* **48** 89

[2] Yan N, Dai F P, Wang W L and Wei B B 2011 *Chin. Phys. Lett.* **28** 078101

[3] Chen C, Chen Z, Zhang J and Yang T 2012 *Acta Phys. Sin.* **61** 108103 (in Chinese)

[4] Du L F, Zhang R, Xing H, Zhang L M, Zhang Y and Liu L 2013 *Acta Phys. Sin.* **62** 106401 (in Chinese)

[5] Coriell S R and Parker R L 1965 *J. Appl. Phys.* **36** 632

[6] Mullins W W and Sekerka R F 1963 *J. Appl. Phys.* **34** 323

[7] Chen Y J, Chen Q, Wang Z D, Hu H Q, Liu Y M and Lian Y D 2004 *J. Tsinghua Sci. Technol.* **44** 1464 (in Chinese)

[8] Buchholz A and Engler S 1996 *Comput. Mater. Sci.* **7** 221

[9] Lv H, Tang S L and Zhou W P 2011 *Chin. Phys. Lett.* **28** 084708

[10] Cao B, Lin X, Wang M and Huang W D 2012 *Chin. Phys. B* **21** 086401

[11] Chen C C, Lin H K and Lan C W 2014 *J. Cryst. Growth* **385** 121

[12] Chen M W, Ni F, Wang Y L, Wang Z D and Xie J X 2011 *Acta Phys. Sin.* **60** 068103 (in Chinese)

[13] Chen M W, Lan M, Yuan L, Wang Y Y, Wang Z D and Xu J J 2009 *Chin. Phys. B* **18** 1691

[14] Zhang Y P, Lin X, Wei L, Peng D J, Wang M and Huang W D 2013 *Acta Phys. Sin.* **62** 178105 (in Chinese)

[15] Galenko P K, Funke O, Wang J and Herlach D M 2004 *Mater. Sci. Eng. A* **375–377** 488

[16] Cao B, Lin X, Wang M and Huang W D 2012 *Chin. Phys. B* **21** 056401

[17] Zhang W and Chen C 2012 *Chin. Phys. Lett.* **29** 084701

[18] Chen M W, Wang B and Wang Z D 2013 *Chin. Phys. B* **22** 116805

[19] Bhattacharyya K and Pop L 2014 *Chin. Phys. B* **23** 024701

[20] Chen M W, Wang Z D, Xie J X and Xu J J 2008 *Acta Mech. Sin.* **24** 681

[21] Chen M W and Wang Z D 2013 *Chin. Phys. B* **22** 098104